Assessment of Turbulence Models for Heavy Liquid Metals in Computational Fluid Dynamics (WP 7 of the ASCHLIM project)

L. Maciocco*

CCT (Centre of Computational Technology, University of Latvia)
CEA (Nuclear Energy Institute, France)
**CRS4 (Centre for Advanced Studies, Research and Development in Sardinia, Italy)*
ENEA (Institute for New Technologies, Energy and Environment, Italy)
FZJ (Juelich Research Centre, Germany)
FZK-IRS (Karlsruhe Research Centre, Germany)
FZR (Rossendorf Research center, Germany)
IPUL (Institute of Physics, University of Latvia)
NRG (Nuclear Research and Consultancy Group, The Netherlands)
PSI (Paul Sherrer Institute, Switzerland)
UPV (University of the Basque Countries, Spain)

December 2002

Summary

A summary and analysis of the results obtained from work-packages 1-6 of the ASCHLIM project is presented in this document, with the aim of defining the performances and shortcomings of CFD turbulence models currently adopted for the simulation of Heavy Liquid Metals flows in nuclear applications.

Two classes of problems are analysed, one related to liquid metals physical characteristics (low Prandtl number) and one related to the flow morphology in typical ADS applications.

Concerning the first class, some drawbacks were found in the use of wall-functions for HLM flows. In fact, thermal wall-functions currently implemented in commercial CFD codes are in general unsuitable for HLM flows, unless the first grid point lays in the thermal sublayer $y^+ < 70 \div 100$.

It was also proved that the Reynolds analogy is not applicable for very low Peclet number flows (~ 100). However, correct results were obtained for higher Pe (~1000), even using a constant value for the turbulent Prandtl number (0.9).

Due to the lack of experimental measurements of turbulence quantities, it was not possible to draw strong conclusions concerning the second class of problems. However, results confirmed the capability of two-equation models to give a reasonably good prediction of the main flow characteristics in complex flow morphology typical of spallation-targets applications. Higher order models, both for momentum and heat turbulence transport, should be used in cases where turbulence anisotropy is important.

Contents

1. Introduction

There is a general consensus in the research institutes and industries working in the field of Heavy Liquid Metals (HLM) on considering Computational Fluid Dynamics (CFD) codes an essential tool for the design of HLM components such as high power spallation targets.

In these devices, a high-energy proton beam interacts with the HLM. The resulting spallation process frees a large quantity of high-energy neutrons. These so-called Spallation Neutron Sources can be an important tool in many fields of physical, material and biological sciences. The spallation process is also at the basis of new techniques for replacing the use of reactors in the production of radioisotopes for medical applications (diagnostic and therapy). The main application of the HLM spallation process can be found in the Accelerator Driven Systems (ADS) aimed at energy production and at transmutation of radioactive waste.

The spallation process produces a large quantity of heat in a very small volume. The best spallation material has been identified by the leading projects in this field (EADF, ESS, MEGAPIE) to be a HLM. Power densities can easily overcome 1000 W/cm^3 not only in the liquid metal, but also in critical structures such as the beam window. Structural materials work at very high temperatures and have to dissipate large quantities of heat. It is fundamental to have a tool capable of simulating the critical phenomena occurring. The physics associated with the spallation can be simulated with the help of a Montecarlo code that, given the complexity of the resulting heat distributions, has to be necessarily coupled with a CFD numerical tool in order to calculate reliable operating conditions for the engineering of these devices.

Turbulence models play a fundamental role in the prediction of temperatures in the structures. In principle, the modelling of a liquid metal flow does not differ from that of any other Newtonian fluid, provided the correct physical properties are used in the governing equations. However, their low Prandtl number makes the turbulent heat transport mechanisms of liquid metals different from those of common fluids like water or air.

Turbulence models commonly used in industrial CFD, as those implemented in commercial codes, present some limitations for the simulation of HLM flows. In fact, models using the turbulent Prandtl number to describe the turbulent heat transport assume the Reynolds analogy, which is not directly applicable to the simulation of heat transfer phenomena in liquid metals. On the other hand, models having a distinct description of the turbulent heat transport contain many parameters whose values, which are determined through both dimensional and empirical analysis, depend both on the type of fluid and on the type of flow. Standard values of these parameters are available for common fluids like gases and water but not for HLMs. Therefore, new model relationships are necessary to extend the validity of the modelled equations to low Peclet numbers.

In general, we can say that there are two classes of problems related to the CFD simulation of liquid metal flows:

- basic limitations of turbulence models (related to the type of flow). In all cases the choice of the model should be based on the characteristics of the flow to be simulated. Experimental tests (even with water) are necessary to test special flow designs (like in the beam target);
- additional limitations related to liquid metal characteristics. In fact, due to their low Prandtl number, liquid metal flows can show different heat transfer mechanisms with respect to

common fluids, especially near walls and in buoyant flows. Therefore, experimental tests are needed even in basic flow configurations (like jets and channels).

In the framework of the ASCHLIM project, six experiments were selected for as many benchmarking activities (corresponding to work packages 1-6) in order to understand the capability of CFD codes to correctly predict turbulence transport phenomena in HLM flows, and to propose possible modifications in order to improve their performances. Different commercial (CFX, Fluent, Star-CD) and in-house (Flutan, Karalis) CFD codes, using various turbulence modelling techniques, were tested on the selected experiments.

2. Summary of the main results from the selected benchmarks

2.1. WP1 - ESS HETSS benchmark [1]

The ESS-HETSS (European Spallation Source - Heat Emitting Temperature Sensing Surfaces) experiment was performed at the Institute of Physics of the Latvian Academy of Science in collaboration with the FZJ research centre of Juelich.

The aim of the ESS mercury target model experiment was to study the heat transfer between a heated surface and a mercury flow, in a flow configuration typical for the ESS spallation target. The test section consists of a bent converging channel. Heat emitting and temperature sensing surfaces (HETSS) were used to apply a constant heat flux from the walls to the mercury flow and to measure the wall temperature. For different flow rates the heat exchange coefficient between the mercury flow and the channel walls was determined. Experimental sensors' temperature were available for comparison with computational results.

A series of numerical simulations were performed with different CFD codes, using different turbulence models and different near-wall treatments. The suitability of wall functions and the eddy diffusivity concept with constant turbulent Prandtl numbers for heavy liquid metal flows was investigated as well as the effect of turbulent anisotropy.

The main benchmark conclusions were the following.

- Numerical results showed a good agreement with experimental data only for the two highest value of the flow rate (namely 1.5 l/s and 1 l/s, corresponding to $Re=2.2 \times 10^5$, $Pe = 5.6 \times 10^3$ and $Re=1.5 \times 10^5$, $Pe = 3.8 \times 10^3$ respectively), the discrepancy increasing with the decreasing of the flow rate (the worse results being obtained at $Re = 1.5 \times 10^4$, $Pe = 3.8 \times 10^2$). This behaviour was noticed independently of the turbulence model used.
- Problems arose while using Wall Functions for the near-wall treatment. In particular:
  - Star-CD wall functions needed to be modified because they do not take into account the different switching position from linear to logarithmic layer between velocity and temperature boundary layer in case of low-Pr fluids.
  - If wall functions are used, y^+ should stay below approximately 70 in order to avoid significant errors for the extrapolated wall temperature. Alternatively the wall temperatures can be extrapolated on the basis of a new correlation $T^*(y^*)$, that is based on the results for the two layer zonal model.

  - In Fluent (Fluent 5 and 6) for low Prandtl number fluids the use of the right thermal law-of-the-wall for the extrapolation of the wall temperature has to be checked.

- Calculations performed with Reynolds Stress and Reynolds Flux models showed that turbulent anisotropy have significant effects on the turbulent heat transport, especially in the second part of the channel bend.
- The deviations for lower flow rates can partly be explained by the heat transferred by conduction from the HETSS to solid walls.
- The standard value for the turbulent Prandtl number (0.85 or 0.9 respectively) give correct results, at least at high flow rates (1 and 1.5 l/s corresponding to $Pe = 3.7 \times 10^3$ and $Pe = 5.6 \times 10^3$ respectively). The influence of the local turbulent Reynolds number on the turbulent Prandtl number, and thus on the temperature profile, is negligible.
- The same simulation performed with different codes, even with identical numerical settings (mesh, convective schemes and turbulence model), can give substantially different results.

2.2. WP2 - TEFLU benchmark [2]

The TEFLU experiment was performed at the Karlsruhe Research Centre (FZK) in order to study the thermal-fluid dynamic behaviour of a hot sodium jet in three different flow regimes (forced convection, buoyant flow, plume). The main aim of this work was the analysis of the applicability of a turbulent-Prandtl-number approach for the modelling of the turbulent transport of energy in the case of fluids with very low molecular Prandtl number (liquid metals).

The TEFLU experimental apparatus allowed the measurement of velocity, temperature and temperature fluctuations. No experimental data were available for velocity fluctuations. This represented a strong limit for the definition of turbulence boundary conditions for the numerical simulation, which makes questionable the evaluation of the capability of turbulence models at predicting the correct jet spreading-rate.

Another problem arises form the intrinsic limitations of turbulence models, which are related to the type of flow to be simulated. In fact, it is well known that almost all the various versions of two-equations models give rise to the so-called round-jet anomaly, consisting in the overestimation of the jet spreading rate.

The main benchmark conclusions were the following.

- Due to computational limitations, none of the participants did discretise the flow in the multi-bore jet block. Therefore, the mixing or spreading results will heavily depend on the turbulence level specified in the inlet conditions into the computational domain, which begins within the spreading area of the multi-jet arrangement. Some inlet conditions were specified in the benchmark description; those were widely used so that only the relative deviations between the different turbulence models could be analysed. Some of the participants used also the modification of the inlet conditions to gain better velocity and temperature spreading rates. Those modifications make direct comparisons impossible.
- The velocity spreading-rate obtained with the prescribed inlet turbulence profiles is overestimated in the forced flow regime. This result is confirmed by all participants but CRS4-CFDC (using a Spalart-Allmaras model) and LAESA (RNG k-ε). Better results are obtained in the buoyant and plume regimes if the assigned profile of ε are used (FZJ, FZK, UPV), while even worse results are obtained by using the extrapolation condition (CRS4-EA, ENEA,

NRG). The reason of it can be found both in the bad performance of two-equation models at predicting round-jets, and in inadequate inlet turbulence boundary conditions.

- The temperature spreading rate is overestimated by all models based on the Reynolds analogy, using $Pr_t = 0.9$. The error is higher in the forced flow regime. Good results are obtained with the TMBF model (FSZ-IRS), which solves equations for the turbulent heat fluxes, and by LAESA. In this last case, it could be due to the strong underestimation of the turbulence field, as it can be deduced from velocity results.
- The comparison between the molecular and the turbulent heat diffusion coefficients calculated with the Reynolds analogy ($Pr_t = 0.9$, CRS4-EA) and with the TMBF model (FZK-IRS), shows that they are of the same order of magnitude, with a prevailing effect of thermal conduction. The value of Pr_t calculated from TMBF results ranges from 2 to 5. However, CRS4-EA obtained the best agreement for temperature profiles with $Pr_t = 10^4$, namely considering only thermal conduction, which would lead to the conclusion that the turbulent heat transfer plays a negligible role in the jet temperature spreading. Definitely, we can conclude that a correct temperature spreading rate can not be obtained using a Pr_t approach with $Pr_t \sim 1$. A more critical check of the other models should be repeated for a flow at larger Reynolds numbers, in which the turbulent heat transfer is more relevant than the molecular one.
- The buoyancy influence in all TEFLU experiments was found in the recalculations to be only weak. So, serious conclusions on the validity of the investigated models for strongly or purely buoyant liquid metal flows can not be drawn from this investigation. From the experience with other fluids it is known that for such flows models are required which record the anisotropy in the turbulent momentum fluxes and which use at least a transport equation for the temperature variances to model thermal stratification phenomena.

2.3. WP3 - COULI experiment & benchmark [3]

The task of the COULI benchmark was the analysis of the capability of turbulence models of simulating a flow configuration typical of the spallation region of the Energy Amplifier Demonstration Facility (EADF) window-type target. This type of target is also considered as the reference one in the framework of the PDS-XADS European project.

The COULI experiment is being carried out at CEA Cadarache. The dimensions of the circuit are scaled by a factor 1/1.4, in geometrical similarity with the EADF target geometry. The experiment is performed with water in isothermal conditions, in fluid dynamic similarity with the Pb-Bi flow in the EADF target. At present, experimental LDV measurements of mean velocity are available in two sections upstream the window region, which are used to set the inlet boundary conditions, and in two sections downstream the diverging duct, for results comparison. Unfortunately, no experimental measurements are available in the actual diverging duct, due to optical problems related to the surface curvature.

Turbulence modelling has been examined with regard to the prediction of the flow characteristics and boundary layer detachment in one particular geometry of a streamlined heavy liquid metal spallation target and for a bulk Reynolds number of about half a million. The investigation concerned the Reynolds stress model (as implemented in Fluent) and various modelling version of the popular k-ε model, with linear or non linear forms of the stress-strain relationship (as implemented in Star-CD). It was also addressed the description of the near wall region, either with

wall functions or with the more elaborate description accounting for the effects of viscosity as the wall is approached (two layer treatment or low Reynolds number treatment).

After the results were confirmed by the usual convergence and grid sensitivity checks, it was found that the predicted mean velocity field had virtually no dependence on the boundary layer treatment but were determined primarily by the turbulence model employed.

Only the Lien quadratic k-ε model and the Chen linear k-ε model were able to predict a significant boundary layer detachment and the resulting recirculation on the target outer wall, as evidenced experimentally by the mean velocity measurements and the flow visualisation on the COULI rig. The "standard" linear k-ε model and more surprisingly the Reynolds stress model failed to do so

Because the final assessment of an actual target in "beam on" conditions requires a large confidence in the CFD prediction, and because a recirculation free streamlining could be the ultimate goal of the design of a liquid metal target, it is worth extending the present validation by:

- comparing with more experimental measurements, especially in sections where boundary layer detachment may potentially occur.
- address the 3D features of the flow, due both to imperfect inlet or geometrical conditions, that will be inevitable anyway in the real target.
- test a different geometry to confirm the promising performance that CFD has shown with the present one, because to be sure of a "no recirculation" prediction , the model must have prove sensitive enough to correctly predict cases with recirculation.

2.4. WP4 - KALLA Rod experiment & benchmark

2.5. WP5 - KALLA Target experiment & benchmark

2.6. WP6 - SINQ HETSS experiment & benchmark

3. Limitations of the Reynolds analogy for HLM flows

The simulation of the turbulent transport of heat in one and two-equations models, as well as in the Reynolds stress model, is based on the Reynolds analogy. According to this approach, the turbulent heat flux is governed by a gradient-diffusion law, analogously to thermal conduction and as it is done for the turbulent transport of momentum within the Boussinesq hypothesis, with a turbulent diffusion coefficient which is proportional to the turbulent viscosity μ_t. The turbulent heat flux vector $q_{t,j}$ is expressed, in tensor notation, as

$$q_{t,j} = \overline{\rho u_j' h'} = -\frac{\mu_t}{Pr_t}\frac{\partial \bar{h}}{\partial x_j} \qquad (1)$$

where u_j is the velocity vector, h the static enthalpy and the prime refers to turbulent fluctuations. The coefficient of proportionality Pr_t between momentum and heat turbulent transport is the turbulent Prandtl number, in analogy with the Prandtl number for molecular transport. Its value is determined empirically on the basis of standard experiments with common fluid like water and air (Pr ~ 1), and is usually set to 0.85 ÷ 0.9.

Besides the basic limitations related to a gradient-diffusion approach, the Reynolds analogy introduces the further hypothesis of direct proportionality between the turbulent transport of momentum and heat. This is reasonable in the cases where the effects of thermal conduction are minor with respect to turbulent heat transfer, as it happens for fully turbulent flows of high-Pr fluids, while it is questionable in case of fluids with low-Pr, like liquid metals, where the effect of thermal conduction can be important even in high-Re flows, especially in zones at low turbulence like near walls.

This problem is taken into account in the RNG k-ε model implemented in FLUENT, where the turbulent Prandtl number is not constant, and is calculated locally through the formula [6]:

$$\left|\frac{Pr_t - 1.3929}{Pr - 1.3929}\right|^{0.6321} \left|\frac{Pr_t + 2.3929}{Pr + 2.3929}\right|^{0.3679} = \frac{\mu}{\mu + \mu_t} \tag{2}$$

that is derived from the RNG theory. This formula gives a smooth transition from the molecular value of the Prandtl number, in low-Re regions (like near walls), to the fully turbulent value (1.393) and, according to [6] gives good results even for very low Prandtl numbers (10^{-2}).

Another formula correlating Pr_t to the fluid/flow characteristics was deduced by Jischa & Rieke on the basis of theoretical and empirical considerations, and is given by [7]

$$Pr_t = c_1 + c_2 \frac{1}{Pr\ Re^m} \tag{3}$$

where c_1 = 0.9, c_2 = 182.4 and m = 0.888 are empirical coefficients. A local form of Eq. (7), expressing Pr_t as a function of the local Prandtl and turbulent Reynolds numbers can be deduced from [7], yielding:

$$Pr_t = c_1 + c_3 \frac{1}{Pr\ Re_t} \tag{4}$$

where c_3 = 0.0899 and

$$Re_t = C_\mu^{-0.25} \frac{\mu_t}{\mu} \tag{5}$$

where C_μ = 0.09. Eq. (8) establishes a relation between Pr_t and the ratio of the turbulent to the molecular viscosity, analogously to Eq. (6).

An alternative method to the Pr_t approach, called Turbulence Model for Buoyant Flows (TMBF) and based on the coupling between a k-ε model and a set of transport equations for the turbulent heat fluxes, was developed at FZK and especially designed for the simulation of low-Pr flows where buoyancy effects are important [8].

The results obtained within the WP2 activity (TEFLU benchmark) [2] showed that, in the case of a round jet of sodium ($Pr \approx 6 \times 10^{-3}$) at $Re \approx 10^4$ (forced jet regime), yielding a Peclet number Pe =

Re Pr ≈ 60, all models based on the Reynolds analogy, with Pr_t =0.9, yield a strong overestimation of the contribution of the turbulent heat flux to the jet thermal spreading rate. Slightly better results, although still not in agreement with experiments, were obtained in the buoyant (Pe ≈ 50) and plume (Pe ≈ 30) regimes.

A good prediction of experimental results was obtained with the TMBF model, which yielded a lower turbulent heat transport. Good results were obtained also using Eq. (7), which in the forced case of WP2 yielded $Pr_t \approx 10$, so resulting in a strong predominance of conduction effects on the turbulent heat transport. However, in all considered flow regimes, the best results were obtained inhibiting the turbulent heat transfer completely, leading to the conclusion that thermal conduction is the only effective heat transport mechanism in the TEFLU jet at all regimes. This explained also the better results obtained for the buoyant and plume regimes even with $Pr_t = 0.9$, thanks to the lower turbulent diffusivity predicted by the codes at these regimes.

The Pr_t field in the TEFLU test section (forced case) calculated with Eq. (8) is shown in Figure 1. It can be seen as a $Pr_t \sim 1$ is predicted in the jet region, which is definitely underestimated according to the results obtained in WP2. It should be also noted that the Pr_t field derived from the calculations with the TMBF model [2] predicted a Pr_t ranging from 2 to 5, which, according to the very good results obtained with $Pr_t = 10$, seems to be underestimated as well. The FLUENT RNG k-ε model, based on Eq. (6), was also tested (FZJ), yielding an almost constant value $Pr_t = 0.85$, and a consequent overestimation of the temperature spreading rate, showing Eq. (6) to be ineffective in this case.

In the case of the Hg (Pr = 0.025) flow in the ESS-HETSS benchmark (WP1), the Peclet number ranges from 370 for the minimum flow rate (0.1 l/s) to 5700 for 1.5 l/s, namely one to two orders of magnitude higher than in the case of the TEFLU jet. However, in this case the heat exchange with a wall is simulated, which implies that regions with low Peclet number exist within the boundary layer (a local Peclet number $Pe_t = Re_t Pr$ can be defined to characterise these regions).

Good results were obtained with $Pr_t = 0.9$ both for 1 and 1.5 l/s, so confirming the validity of the Reynolds analogy at these regimes. A bad agreement with experimental data was found at lower flow rates, due to other problems not directly related to the use of the Reynolds analogy, which do not allow to draw definite conclusions about the validity of the Pr_t approach at these Pe.

Two simulation, at 0.1 and 1.5 l/s, were performed using the FLUENT RNG k-ε model, so applying Eq. (6) for the calculation of Pr_t, and the resulting profiles of Pr_t in different cross sections showed a very low variation (order 0.5 %) from the bulk value of 0.85.

In the case of the ESS-HETSS benchmark, Eq. (7) yields a Pr_t ranging from 1 at 1.5 l/s to 2.3 at 0.1 l/s, so getting the correct order of magnitude. The distribution of Pr_t, calculated with Eq. (8), on the symmetry plane of the ESS-HETSS test section for the two cases at q = 1 l/s and q = 0.1 l/s is shown in Figure 2, and the resulting HETSS temperatures are plotted in Figure 3. A Pr_t significantly higher than 0.9 can be found only in the very vicinity of the wall, where thermal conduction is already predominant; hence, the effect of the Pr_t variation results to be minor even at low flow rates.

From the above results, it can be concluded that the Reynolds-analogy approach with $Pr_t = 0.85 \div 0.9$ is suitable for the simulation of the heat exchange in HLM flows with Pe > ~ 1000, while it can not be used for Pe ~ 100. The two approaches based on the use of a locally variable Pr_t, as a

function of Pr and of the turbulent to molecular viscosity ratio, namely Eq. (6) and Eq. (8), failed in giving correct results for very low Peclet numbers. Eq. (7) yielded a reasonable estimation of the magnitude of Pr_t in both the considered cases, and can probably be used as an indicator of the importance of low-Pectlet number effects.

The use of models not based on the Reynolds analogy, like the TMBF model, can be a safer approach, although computationally more expensive, to the simulation of low-Pe flows. However, the results available within the ASCHLIM project are not sufficient to evaluate the actual performances of the TMBF.

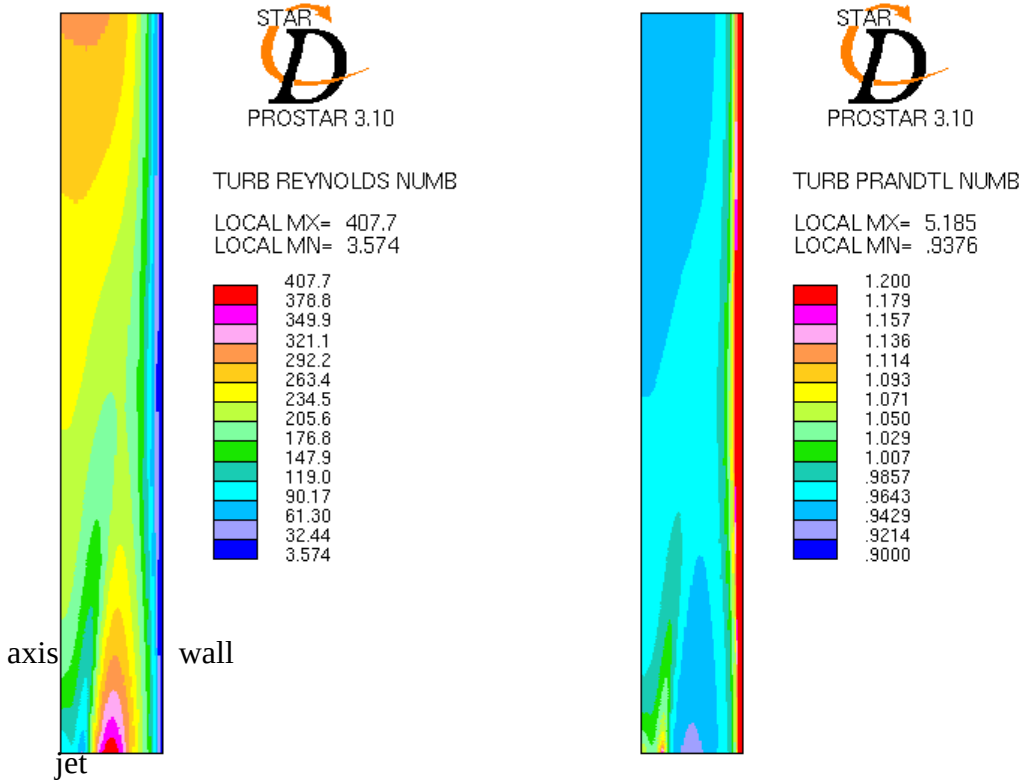

Figure 1 - Example of distribution of turbulent Reynolds number (left) and Prandtl number (right), calculated with Eq. (8), in the TEFLU test section for the forced case (Star-CD, Chen k-ε).

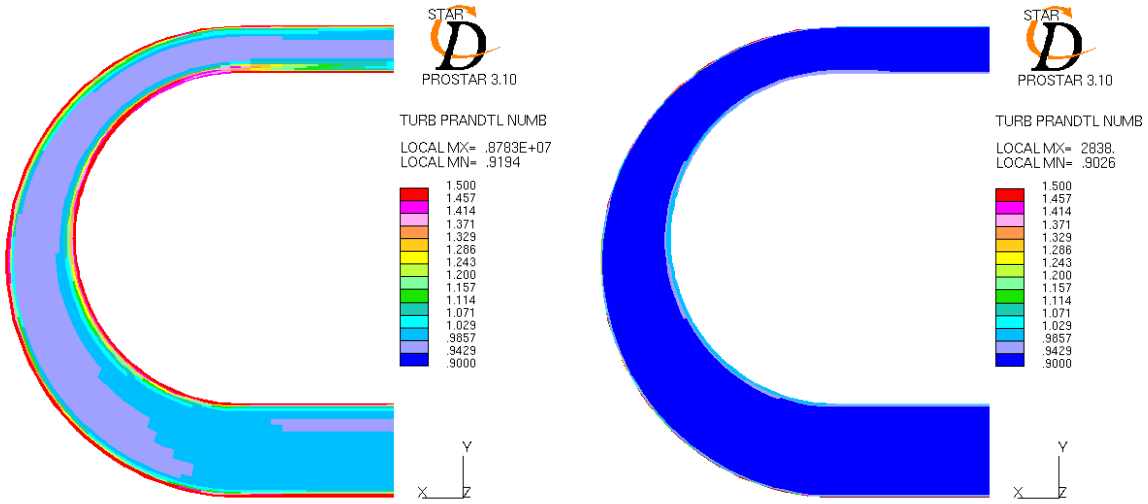

Figure 2 - Example of distribution of Pr_t, calculated with Eq. (8), in the ESS-HETSS test section for q=0.1 l/s (left) and q= 1 l/s (right) (Star-CD, Standard k-ε with Two-Layer).

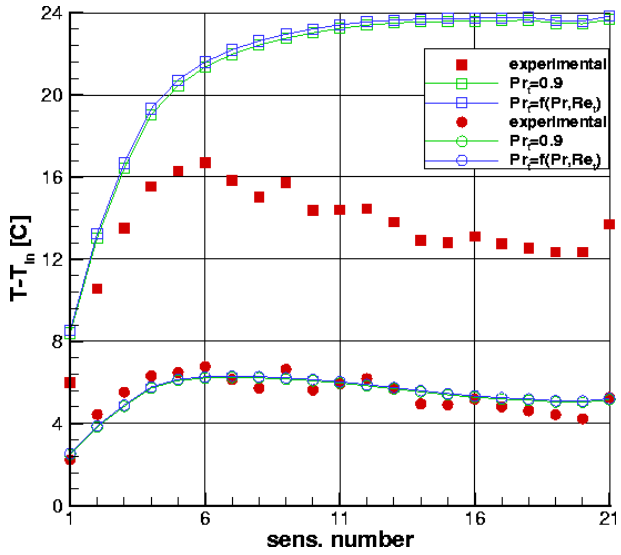

Figure 3 - Comparison of HETSS temperatures obtained with Pr_t = 0.9 and Pr_t calculated with Eq. (8) for 0.1 l/s (square symbols) and 1 l/s (circles).

4. Application of Wall Functions in HLM flows

The Wall Function (WF) method is widely used in industrial CFD applications to solve the problem of near-wall turbulence while using high Reynolds number turbulence models. It is based on the so-called "universal law of the wall", which prescribes a logarithmic profile for the velocity boundary layer under the following assumptions [4]:

- flow-variables gradients normal to the wall are predominant (one dimensional behaviour);
- negligible effects of pressure gradients and body forces in the boundary layer (uniform shear stress);

- shear stress and velocity vector are aligned and unidirectional throughout the layer
- balance between turbulence energy production and dissipation;
- linear variation of turbulence length scale.

In principle these assumptions are verified only for very basic flows, like the flow on a flat plate or in a pipe without adverse pressure gradients. However, this approach can give reasonable results (at least from the engineering point of view) even for more complex flows, unless too far from the basic assumptions, and it has the big advantage of reducing considerably the mesh size.

In the WF approach, the velocity boundary layer is divided in two layers: the viscous sub-layer, where viscous effect are predominant and, due to the assumption of constant shear stress, the velocity profile is linear, and the logarithmic layer, where the universal log-law applies. This is expressed in non-dimensional form as

$$u^+ = \begin{cases} y^+ & y^+ \le y_m^+ \\ \frac{1}{\kappa}\ln(E\, y^+) & y^+ > y_m^+ \end{cases} \tag{6}$$

where u^+ and y^+ are the velocity (parallel to the wall) and the normal distance from the wall, non-dimensionalised through the shear stress at the wall [4][5][6], and κ and E are empirical constants (usually set to 0.4÷0.42 and to 9÷9.8 respectively). The transition distance y_m^+ is determined by equating the two expressions (yielding a value of about 11.5 with the commonly used values κ=0.4 and E=9).

Temperature wall functions are deduced in analogy with velocity wall functions. In all the three major commercial codes, namely CFX (version 4.2) [5], FLUENT [6] and Star-CD (version 3.1) [4], the implementation of temperature wall functions is analogous, although some basic differences exist, as explained below. In general, they are expressed as

$$T^+ = \begin{cases} Pr_t\, y^+ & y^+ \le y_T^+ \\ Pr_t\left[\frac{1}{\kappa}\ln(E\, y^+) + P\right] & y^+ > y_T^+ \end{cases} \tag{7}$$

where T^+ is the non-dimensional temperature, Pr_t the turbulent Prandtl number and y_T^+ is the switching position from linear to logarithmic behaviour, deduced from the intersection of the two profiles. P is the so-called sublayer resistance factor, which takes into account the different thickness of the conduction sublayer with respect to the viscous sublayer for fluids with $Pr \neq 1$, and whose expression as a function of the molecular and turbulent Prandtl numbers is given further on.

The main implementation differences in the three considered codes are the following.

- Star-CD does not consider a different switching position for the velocity and the temperature layers, and always uses the expression

  $$T^+ = Pr_t(u^+ + P)$$

  therefore switching from linear to log behaviour at y_m^+. This is surely incorrect in the case of low-Pr fluids like liquid metals, where thermal conduction is dominant in a much thicker layer than the viscous one. The error deriving from this approach has been put in evidence within WP1 (ESS-HETSS benchmark, see Sec. 2.1), resulting in a strong overestimation of HETSS temperatures even at high flow rates, where the other codes' wall functions performed

reasonably well (even if other problems arose, as discussed below). Formulation (2) was implemented through user subroutine, yielding results in line with the other codes [1].

- In Star-CD and CFX, the Jayatilleke expression for P is used, namely:

$$P = E_1 \left[\left(\frac{Pr}{Pr_t} \right)^{0.75} - 1 \right] \left[1 + 0.28 \exp\left(-0.007 \frac{Pr}{Pr_t} \right) \right] \tag{8}$$

where E_1 = 9.24 in Star-CD and E_1 = 9 in CFX. FLUENT 5 adopt a different expression, by Launder & Spalding, which reads

$$P = \frac{\pi/4}{\sin(\pi/4)} \left(\frac{26}{\kappa} \right) \left(\frac{Pr}{Pr_t} - 1 \right) \left(\frac{Pr_t}{Pr} \right)^{0.75} \tag{9}$$

These two expressions give almost the same values for Pr ~ 1, similar values for Pr > 1 but very different values for Pr << 1 as in our case (for Pr = 0.02 and using Pr_t = 0.9, Eq.(3) gives P = -11.1, Eq. (4) gives P = -22.6). It is shown in [1] that no intersection exists in FLUENT 5 between the linear and log profiles for Pr = 0.025, so that the linear law is used independently of the value of y^+. According to the results of WP1, FLUENT 6 has a different wall function implementation, probably using Eq. (3) instead of Eq.(4), as done in CFX.

- Some additional terms in Eq. (2) taking into account the effect of viscous dissipation at high velocities are implemented in FLUENT, which should be ineffective for HLM applications here considered.

The two curves obtained with Eq. (2) and Eq. (3), assuming Pr_t = 0.9, are plotted in Figure 4. It can be seen that the value of y_T^+, namely the intersection between linear and log profiles, is about 250 for Pr=0.03 and about 460 for Pr=0.02 (values typical of Pb-Bi and Hg), while no intersection is found for Pr=0.006 (Na). Considering that the upper value of y^+ momentum wall-functions are considered applicable for is about 300, and that a reasonably accurate mesh for the applications considered here usually does not yields y^+ values larger than about 200, the use of Eq. (2) and Eq. (3) results in the application of a linear temperature profile in the majority of cases where HLM flows are simulated.

However, a comparison between results obtained with wall-functions and two-layer models in WP1, showed that, for Pr = 0.025, the temperature profiles predicted with the two-layer become linear at $y^+ \cong 70$, with an acceptable error up to $y^+ \cong 100$, while a switching position $y_T^+ \cong 250$ results from Eqs. (2) and (3).

It should be noted that all the above consideration are based on the use of Pr_t = 0.9 in Eqs. (3) and (4). As explained in Sec. 3, this value can be too low for liquid-metal flows; however, as it can be deduced from Eq. (2) and Eq. (3), an increase of Pr_t would results in an increase of y_T^+, and therefore to a further extension of the linear thermal sublayer.

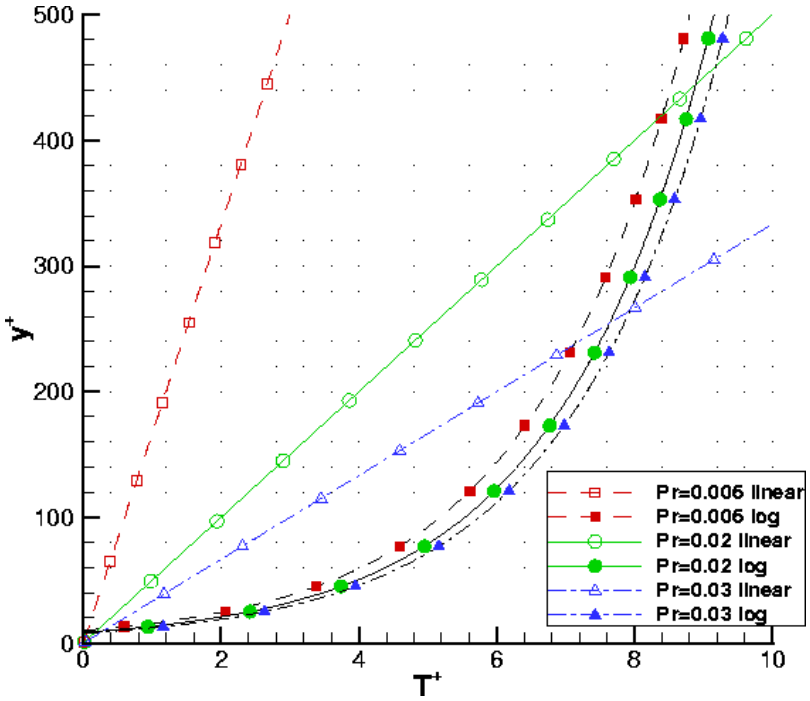

Figure 4 - Thermal wall functions, according to Eqs. (2) and (3), for different values of the Prandtl number: Pr=0.006 corresponds to Sodium at 300 °C, Pr=0.02÷0.03 to Mercury and Lead-Bismuth in the range 300 ÷400 °C

In conclusion, thermal wall-functions currently implemented in commercial CFD codes seem to be unsuitable for general applications with liquid metals flows, unless the value of y^+ is kept below 100 in all near-wall regions where the heat exchange with the wall, or wall temperatures corresponding to a given heat flux, has to be predicted.

5. Problems related to the flow morphology

Besides the problems related to HLM physical characteristics, the intrinsic limitations of turbulence models must be taken into account. In fact, the reliability of the prediction of the flow characteristics, and therefore of the heat transport mechanisms, strongly depends on the suitability of the chosen model to face the considered flow morphology.

The performances of turbulence models based on Reynolds-averaged Navier-Stokes equations (one and two-equations models, Reynolds stress models) are strongly related to the flow characteristics. Although their limits of applicability are in general known, their actual performances in specific applications are influenced by many factors, like:

- implementation in CFD codes. Slightly different versions of the same model can be found in different codes, or different values of model's constants can be adopted. Furthermore, even if exactly the same model with the same constants' value is used, different codes can give different results for the same application. A demonstration of this fact was shown within WP1 [1].
- Combination between turbulence model and turbulence boundary conditions on solid walls. Apart from the low-Reynolds versions of the k-ε and k-ω models and from the Spalart-Allmaras model, all the other models need to be joined with some modelling of near-wall low-

Re effects. Basically, two approaches are available in commercial codes, namely Wall-Functions, already discussed in Sec. 4, and Two-Layer models [4][6]. The effect of the chosen near-wall treatment can be very strong on turbulence-model performances.

- Complexity of the flow morphology. The limits of applicability of turbulence models are usually known for basic flows like boundary and shear layers, steps, blunt or sharp bodies in a stream etc. More complex flows can be usually seen as a combination of basic flow, so that some indications about the possible performances of a turbulence model can be deduced. However, in order to be sure about the reliability of the results for complex flows, an assessment on the considered flow morphology is necessary.
- CFD model set-up. The quality of the computational mesh and the accuracy of the convective schemes adopted can be crucial for a realistic prediction of complex flow patterns. Furthermore, a correct description of turbulence characteristics at inlet boundary conditions can strongly influence the results.

Some useful indications came from the ASCHLIM benchmarking activity concerning the performances of the most used turbulence models on applications typical of ADS systems (see also Sec. 2).

One of the possible drawbacks can be a strong turbulence anisotropy. In fact, turbulence models based on the Boussinesq eddy-viscosity approximation [9], assume isotropic turbulence characteristics (defined by the scalar quantity μ_t), while they can be different in different directions, depending on the flow characteristics. The ESS-HETSS benchmark (Sec. 2.1) put in evidence the effects of flow anisotropy, generated by the duct curvature, on the evaluation of the heat exchange with the heated wall. In fact, the disagreement between computed and experimental results at lower flow rates was partially compensated using the Reynolds Flux Model (RNF) [5], which couples a Reynolds Stress model (RNS), which is still based on Eq. (5), to the solution of transport equations for turbulent heat fluxes (Reynolds fluxes) [5]. However, a very high computational effort is required by the RNF model, which can be a problem for the simulation of more complex devices. Furthermore, due to the modelling assumptions contained in their equations, RNS and RNF models do not show better performances than two-equations models for all classes of flows [6].

An alternative to the Boussinesq approximation is given by non-linear models, where the Reynolds stresses components are modelled as a function of μ, k, ε and of the mean strain and vorticity tensors. However, at least in the version implemented in Star-CD [4], Reynolds fluxes are still modelled according to Eq. (5), therefore not taking into account anisotropy effects. It is shown in [1] that the use of a quadratic k-ε model does not improve the prediction of sensors' temperature at low flow rates in the ESS-HETSS benchmark. Better results could be probably obtained in this case by using the TMBF model [8], which however was not used within WP1.

Another benchmark where turbulence anisotropy could play a significant role was the COULI isothermal flow (WP3, Sec. 2.3), which is characterised by the presence of a stagnation point (the window) and a strong flow curvature with adverse pressure gradient, yielding a flow-detachment region. In this case both the turbulence model and the near-wall treatment could play an important role on the definition of the flow pattern. Furthermore, models behaviour when approaching the stagnation point is determinant for the correct simulation of the flow in the curved-diverging duct, whose features heavily depend on the turbulence characteristics generated upstream.

As shown in [3] (see also Sec. 2.3), wall functions gave results analogous to those obtained with a two-layer or low-Re approach, even if the normal equilibrium wall functions were used (non-equilibrium wall functions also exist, aimed at solving flows with adverse pressure gradients [6]).

The influence of the bulk turbulence modelling was found to be much stronger. In fact, the Standard k-ε showed its known tendency to overestimate the turbulence production near stagnation points, resulting, in the case of the linear version, in the overestimation of turbulence level in downstream sections, with no boundary layer detachment on the external wall. This tendency seems to be compensated in non-linear versions, which showed to be able to predict the flow detachment, even if a (probably) abnormal peak of turbulence energy is still generated in the internal part of the duct. Satisfactory results were obtained using the Chen k-ε [10]; however, it seems to underestimate more than the other models the turbulence diffusion along the riser (even if the large range of variation of experimental profile could make this last consideration questionable). Surprisingly, the results obtained with the RNS model appear to be quite poor; however it is likely due to the fact that a too coarse mesh coupled with a first-order scheme was used, pointing out the importance of the mesh and convective schemes adopted.

In general, two-equations models showed to be able to reproduce correctly the main flow characteristics. However, the use of the Standard k-ε model (at least in its linear version) in cases with large stagnation points should be avoided.

Some interesting indications came also from the TEFLU benchmark (Sec. 2.2). In fact, even if it is one of the basic flow turbulence models are validated on, it is very challenging for two-equations models due to the well-known round-jet anomaly, that is an overestimation of the jet velocity spreading rate [9]. Even if the problem of the inlet boundary conditions did not allow a proper evaluation of the performances of the models adopted, some relative conclusions could be drawn. A comparison between various version of the k-ε model implemented in Star-CD, showed that the lowest spreading rate was obtained with the Chen k-ε. Non-linear models gave the largest spreading rate, and even the RNG k-ε seem to perform worse than the Standard k-ε in this case.

This confirms the well-known conclusion that the best choice of the model depends on the considered application. However, it is worth to remark that, compatibly with the basic limitations of two-equations model, the Chen k-ε gave very good results in all the considered applications.

6. Conclusions

A summary and analysis of the results obtained from work-packages 1-6 is presented in this document, with the aim of defining the performances and shortcomings of CFD turbulence models currently adopted for the simulation of Heavy Liquid Metals flows in nuclear applications.

From the point of view of momentum turbulent transport mechanisms, no basic differences exist between HLM and common fluids like water and air. Therefore, in those cases where the dynamic and thermal fields are not strictly linked, like in flows where buoyancy plays an important role, no further drawbacks are introduced in the correct simulation of the flow pattern, beyond the standard limitations intrinsic to all turbulence models. These must be carefully take into account in any case when choosing the turbulence model for the considered application. Due to the lack of experimental measurements of turbulence quantities, it was not possible to draw strong conclusions about this point. However, results from the COULI benchmark confirmed the capability of two-equation models to give a reasonably good prediction of the main flow characteristics in complex flow morphology typical of spallation-targets applications. Among the tested two-equations turbulence models, the Chen k-ε showed a high standard of performance in all the considered applications. Higher order models, both for momentum and heat turbulence transport, should be used in cases where turbulence anisotropy is important, like in the ESS-HETSS bent channel at lower Reynolds ($\sim 10^4$).

The important peculiarity of HLM regarding turbulence modelling is their low Prandtl number. The most common modelling approach to the simulation of turbulent heat transport in CFD turbulence models is based on the direct proportionality between the turbulent transport of momentum and heat (Reynolds analogy). It was proved that this is in general not true for HLM. In fact, it was shown that the turbulent Prandtl number approach with a constant $Pr_t = 0.9$ overestimate the turbulent heat transport in flows with Peclet numbers of order 100, although it seems acceptable for Pe ~1000, unless wide regions with a low Re_t (and therefore low Pe_t) exist in the flow domain. Some expression of the turbulent Prandtl number as a function of local turbulence characteristics were considered; however, they failed in very low Peclet flows (TEFLU) and were almost ineffective at higher Pe (ESS-HETSS). A more accurate analysis is still necessary in order to set the exact range of applicability of the Reynolds analogy, and to understand if a general expression of a local $Pr_t = f(Pr, Re_t)$ can be found to extend the capabilities of Pr_t-based models of simulating HLM flows.

An alternative approach was tested, based on the coupling between a k-ε model and a set of transport equations for the turbulent heat fluxes (TMBF), so overcoming the Reynolds analogy while keeping reasonable the computational cost. Although good results were obtained in the TEFLU benchmark, a more extensive testing should be necessary to estimate its actual capabilities.

Some drawbacks were found in the use of wall-functions for HLM flows. In fact, thermal wall-functions currently implemented in commercial CFD codes are in general unsuitable for HLM flows, unless the first grid point lays in the thermal sublayer dominated by molecular conductivity. The condition for this, according to calculations carried out with a two-layer approach, is that the value of y^+ is kept below $70 \div 100$. Even in this case, wall functions implemented in Star-CD must be modified in order to set a different switching position from linear to logarithmic behaviour for the temperature layer with respect to the velocity layer. An alternative law-of-the-wall has been proposed for $y^+ > 70$ which, however, should be confirmed by experimental validation.

A final consideration can be done about the effect of the low Pr of HLM on the buoyancy turbulence production. Unfortunately, the benchmarks carried out could not give useful information about this point, due to the very scarce effect of turbulent heat transport (especially in buoyant regimes) and to the uncertainties in the inlet conditions in the case of the TEFLU, due to the scarce effects of buoyancy in the case of the ESS-HETSS. However, taking into account that the generation of turbulence due to buoyancy is proportional to local temperature gradients, which in low-Pr are smoothed down by the high thermal conductivity, it can be qualitatively concluded that these effects are less important for liquid metals.

7. Guidelines for future activities

Some important indications about the use of CFD turbulence models have come from the ASCHLIM benchmarking activity, although in some cases only partial conclusions could be drawn, principally due to the lack of experimental measurements of turbulence quantities.

The most important point to be clarified is the exact range of applicability of the turbulent Prandtl number approach to HLM flows, and possibly to extend it through the formulation, if exists, of a relationship between Pr_t and the local fluid and flow characteristics (e.g. Pr and Re_t), valid at least in the range of Peclet numbers of interest for ADS applications. The THESYS experimental set-up (WP 4) can be a precious instrument to score this goal. In fact it gives the possibility to study basic turbulent heat-transfer mechanisms in a wide range of Peclet numbers, supplying both for measurements of wall heat fluxes and for measurements of velocity, temperature and their fluctuations in the bulk flow. A further miniaturisation of the measuring probe would allow performing measurements within the boundary layer, so giving also the possibility to study local low-Re (low Pe) effects. These data could also be used to formulate thermal wall functions for liquid metals valid in the non-linear region above y^+~100. The collaboration of commercial CFD codes developers would be very important to reach this task.

More precise indications about the capability of turbulence models to simulate flow morphologies typical of ADS application can still be deduced from the COULI experiment (WP3), once measurements of turbulence quantities are available and if a correction to the flow apparatus will be done to make the flow axisymmetric.

The KALLA (WP5) and SINQ-HETSS (WP6) facilities are a very challenging test bench, where the capabilities of CFD codes, joined with the experience coming from the ASCHLIM project and with the proposed further development, can be entirely tested.

8. References

[1] J. Wolters (FZJ, WP1 coordinator), CRS4, FZJ, IPUL, NRG, PSI, "*ESS-HETSS Computational Benchmark*", December 2002

[2] L. Maciocco (CRS4, WP2 coordinator), ENEA, FZJ, FZK, LAESA, NRG, UPV, "*TEFLU Computational Benchmark - ASCHLIM Project, WP2"*, June 2002

[3] P. Roubin (CEA, WP3 coordinator), CRS4, NRG, UPV, *"COULI Computational Benchmark - ASCHLIM Project, WP3*", December 2002

[4] "*Star-CD v3.05 User Manual*", Computational Dynamics Limited, 1998.

[5] "*CFX –4.2 Solver Manual"*, AEA Technology, 1997

[6] "*FLUENT 4 - User's Guide*", FLUENT Inc., 1997, "*FLUENT 5 - User's Guide*", FLUENT Inc., 1998

[7] M. Jisha, H.B. Rieke, "*Modeling assumptions for turbulent heat transfer*",

[8] L.N. Carteciano, D. Weinberg, U. Müller, "*Development and Analysis of a turbulence model for buoyant flows*", 4th World Conference of Exp. Heat Transfer, Fluid Mechanics and Thermodynamics, Bruxelles, June 1997, Vol. 3, pp. 1339-1347

[9] D. C. Wilcox, "Turbulence Modelling for CFD", DCW Industries, Inc., 1994.

[10] Y.S. Chen, S.W. Kim, "*Computation of turbulent flows using an extended k-ε turbulence closure model*", NASA CR-179204, 1996